Polymer xxx (2014) 1–13

Contents lists available at ScienceDirect

Polymer

journal homepage: www.elsevier.com/locate/polymer

Conformational characteristics and configurational properties of poly(ethylene succinate) and poly(butylene succinate) and structure–property–function relationships of representative biodegradable polyesters

Yuji Sasanuma*, Yuta Nonaka, Yuki Yamaguchi

Department of Applied Chemistry and Biotechnology, Graduate School and Faculty of Engineering, Chiba University, 1-33 Yayoi-cho, Inage-ku, Chiba 263-8522, Japan

ARTICLE INFO

Article history:
Received 20 August 2014
Received in revised form
30 October 2014
Accepted 1 November 2014
Available online xxx

Keywords:
Poly(ethylene succinate)
Poly(butylene succinate)
Conformational analysis

ABSTRACT

Conformational characteristics and configurational properties of synthetic biodegradable polyesters, poly(ethylene succinate) and poly(butylene succinate), have been investigated by NMR experiments and molecular orbital calculations on their model compounds and the rotational isomeric state calculations for the two aliphatic polyesters. The results have been related to their crystal structures and thermal properties and compared with those obtained previously for poly((*R*)-3-hydroxybutyrate) and poly(lactic acid) to elucidate structure–property relationships of the representative biodegradable polyesters. In addition, selective affinities to degradative enzymes of the four polyesters have been satisfactorily explained in terms of their conformational characteristics and interactions with the depolymerases.

1. Introduction

Biodegradable polyesters may be classified into three types: natural, semi-natural, and synthetic polyesters. Poly((*R*)-3-hydroxybutyrate) (PHB) is a purely natural polyester, because it is synthesized and decomposed by microorganisms [1]. Poly(lactic acid) (PLA) is artificially produced from carbon-neutral lactic acid or lactide [2]. Poly(ethylene succinate) (PES, Fig. 1b) and poly(butylene succinate) (PBS, Fig. 1d) are produced from petrochemicals such as succinic acid, dimethyl succinate, ethylene glycol, and 1,4-butanediol [3,4]. These chemicals will be derived from carbon-neutral resources in the future.

In previous studies [5,6], we investigated conformational characteristics and configurational properties of PHB and PLA and elucidated their solution properties, crystal structures, crystallization behaviors, and interactions with degradative enzymes. This study has dealt with PES and PBS: Conformational preferences of the skeletal bonds have been revealed through NMR experiments and molecular orbital (MO) calculations on their small model compounds and related to crystal structures of the two polyesters. Conformational free energies, evaluated from the MO calculations and established through comparison with the NMR experiments, were applied to the refined rotational isomeric state (RIS) scheme [7–9] to derive configurational properties and thermodynamic quantities of PES and PBS, compare them with those of PHB and PLA, and clarify differences between the four biodegradable polyesters. As will be stated below, it is known that these polyesters are selectively degraded by specific microorganisms and enzymes. The selectivity is also treated herein to be explained in terms of the conformational characteristics of the polyesters.

Tokiwa et al. [1,10–14] have investigated biodegradation behaviors of various polyesters including PHB, PLA, PES, and PBS under different conditions with a number of microorganisms and purified degradative enzymes to find the following facts: (1) The populations of polymer-degrading microorganisms can be estimated to be in the order of PHB > PBS > PLA. (2) In the natural environment, PHB-degraders are widely distributed among families of *Pseudonocardiaceae* and related genera, *Micromonosporaceae*, *Thermonosporaceae*, *Streptosporangiaceae*, and *Streptomycetaceae*. (3) Lipases hydrolyze aliphatic polyesters with relatively many methylene groups, *e.g.*, poly(ε-caprolactone), poly(ester carbonate), PES, and PBS but are incapable of degrading optically active polyesters such as PHB and PLA. (4) A serine protease, proteinase K, which selectively cleaves the Ala–Ala linkage of

* Corresponding author. Tel./fax: +81 43 290 3394.
E-mail address: sasanuma@faculty.chiba-u.jp (Y. Sasanuma).

http://dx.doi.org/10.1016/j.polymer.2014.11.003
0032-3861/

silk fibroins, can also effectively degrade PLA. This may be partly because of the similarity in chemical structure between alanine and lactic acid. (5) The melting point of the polyesters is closely related to the enzymatic degradability.

This study has also aimed to interpret the above microbiological findings in terms of polymer physicochemistry.

2. Methods

2.1. Sample preparation

Commercial available chemicals were used as received: ethylene glycol, 1,4-butanediol, acetyl chloride, diethyl ether, 1,4-dioxane, ethyl acetate, *n*-hexane, silica gel (Wako Pure Chemical Industries, Tokyo, Japan); succinyl chloride, acetyl chloride-^{13}C (Sigma–Aldrich Japan, Tokyo, Japan).

All syntheses here employed the following experimental setup: a four-necked flask (under a stream of dry nitrogen) equipped with a mechanical or a magnetic stirrer and a Dimroth condenser connected to a calcium chloride drying tube. In silica gel column chromatography, a mixed eluting solvent (ethyl acetate:*n*-hexane = 1:1) was used. All products were identified by NMR.

2.1.1. Dimethyl succinate (DMS)

Methanol (2.7 mL, 67 mmol) was added to succinyl chloride (3.0 mL, 27 mmol) and stirred for 1 h. After methanol (1.0 mL, 25 mmol) was superadded, the mixture was gradually heated up to 70 °C, kept there for 1 h to remove generated hydrogen chloride, and then cooled down to ambient temperature. After pyridine (1.1 mL, 14 mmol) was added, the reaction mixture was stirred, filtrated, and condensed on a rotary evaporator to yield DMS.

2.1.2. Ethylene glycol diacetate (EGDA)

Acetyl chloride (4.5 mL, 63 mmol) was added to ethylene glycol (1.97 g, 32 mmol) and pyridine (5.03 g, 64 mmol) stirred in the four-necked flask, and then the mixture was stirred for 3 h with the flask bathed in ice water. Diethyl ether was added into the flask, and the mixture was filtrated to remove white precipitate. The filtrate was subjected to the silica gel column chromatography (R_f of the product ~ 0.6) and condensed to yield EGDA (yield 32%).

2.1.3. Ethylene glycol diacetate-^{13}C (EGDA-^{13}C)

Acetyl chloride (30 mL, 0.42 mol) was added to ethylene glycol (31.4 g, 0.51 mol) dissolved in 1,4-dioxane (52 mL, 0.61 mol) stirred in the four-necked flask. The mixture was refluxed for 2 h with the flask heated at 120 °C in an oil bath [15]. After cooled down to ambient temperature, the reaction mixture was condensed and purified by the column chromatography (R_f of the product ~ 0.3) to yield ethylene glycol monoacetate (yield 42%).

Acetyl chloride-^{13}C (0.25 g, 3.1 mmol) was added to a mixture of ethylene glycol monoacetate (0.43 g, 4.1 mmol) and pyridine (0.32 g, 4.1 mmol) and stirred for 3 h. The handling described in Section 2.1.2 was employed to yield EGDA-^{13}C (56%).

2.1.4. Ethylene glycol di(methyl succinate) (EGDMS)

This compound was prepared according to van der Brand et al. [16].

2.1.5. Butylene glycol diacetate (BGDA)

Acetyl chloride (5.0 mL, 70 mmol) was added to 1,4-butanediol (3.8 g, 42 mol) and pyridine (6.7 g, 85 mmol) in the flask kept at 0 °C, and then the mixture was stirred at 0 °C for 3 h. Diethyl ether was added into the flask, and yellow solid was precipitated and removed by filtration. The filtrate (2 mL) underwent extraction with ethyl acetate (100 mL) and water (100 mL), and this extraction was repeated four times. The organic layer was condensed and subjected to the column chromatography (R_f of the product ~ 0.6, yield 26%).

2.1.6. Butylene glycol diacetate-^{13}C (BGDA-^{13}C)

Acetyl chloride (5.0 mL, 70 mmol), 1,4-butanediol (7.6 g, 84 mmol), and pyridine (6.7 g, 85 mmol) were treated in the same manner as described in Section 2.1.5 to yield butylene glycol monoacetate (R_f of the product ~ 0.3, yield 25%).

Acetyl chloride-^{13}C (0.25 g, 3.1 mmol) was added to butylene glycol monoacetate (0.51 g, 3.9 mmol) and pyridine (0.30 g, 3.8 mmol), and the mixture was stirred at 0 °C for 3 h and purified as described in Section 2.1.2 to yield BGDA-^{13}C (64%).

2.2. NMR measurements

^1H (^{13}C) NMR spectra were recorded at 500 MHz (125.7 MHz) on a JEOL JNM-ECA500 spectrometer equipped with a variable temperature controller in the Center for Analytical Instrumentation of Chiba University. The measurement temperatures were 15, 25, 35, 45, and 55 °C and maintained within ±0.1 °C fluctuations. Free induction decays (FIDs) were accumulated 32 (256) times. The π/2 pulse width, data acquisition time, and recycle delay were 5.6 (5.0) μs, 3.3 (2.0) s, and 3.7 (2.0) s, respectively. In the ^{13}C NMR experiments, the gated decoupling technique was employed under the conditions given in the above parentheses. The solvents were cyclohexane-d_{12} (C_2D_{12}), benzene-d_6 (C_6D_6), chloroform-d ($CDCl_3$), methanol-d_4 (CD_3OD), and dimethyl-d_6 sulfoxide ($(CD_3)_2SO$), and the solute concentration was approximately 5 vol%. The NMR spectra were simulated with the gNMR program [17] to yield chemical shifts and coupling constants.

2.3. MO calculations on model compounds

Density functional and *ab initio* MO calculations were carried out with the Gaussian09 program [18] installed on an HPC Systems 5000-Z800 computer. For each conformer of model compounds, the geometrical parameters were fully optimized at the B3LYP/6-311+G(2d,p) level, and the thermal-correction term to the Gibbs free energy (at 25 °C) was calculated at the same level. Bond lengths, bond angles, and dihedral angles used in the refined RIS computations were chosen from the optimized geometrical parameters (see Tables S4 and S5, Supplementary data). All the self-consistent field calculations were conducted under the tight convergence. With the optimized geometry, the electronic energy was computed at the MP2/6-311+G(2d,p) and M062X/6-311+G(2d,p) level [19]. The Gibbs free energy was evaluated from the electronic energy and the thermal-correction term, being given here as the difference from that of the all-trans conformer and denoted as ΔG. Vicinal $^1H-^1H$ and $^{13}C-^1H$ coupling constants used to determine bond conformations of model compounds were calculated at the B3LYP/6-311++G(3df,3pd) level [20]. The ΔG values of the model compounds in benzene and chloroform at 25 °C were also calculated at the MP2/6-311+G(2d,p) and M062X/6-311+G(2d,p) level with the integral equation formalism of the polarizable continuum model [21].

Herein the dihedral angle is defined according to the tradition in polymer science [7]: trans (t) ~±0°, cis (c) ~±180°, gauche$^+$ (g$^+$) ~+120°, and gauche$^-$ (g$^-$) ~−120°. The dihedral angle (ϕ) can be converted to that (Φ) recommended by IUPAC [22] according to $\Phi = -\mathrm{sign}(\phi)(180 - |\phi|)$, where the function, sign(ϕ), returns the sign of ϕ, and *vice versa*: $\phi = -\mathrm{sign}(\Phi)(180-|\Phi|)$. Non-SI units are

Please cite this article in press as: Sasanuma Y, et al., Conformational characteristics and configurational properties of poly(ethylene succinate) and poly(butylene succinate) and structure–property–function relationships of representative biodegradable polyesters, Polymer (2014), http://dx.doi.org/10.1016/j.polymer.2014.11.003

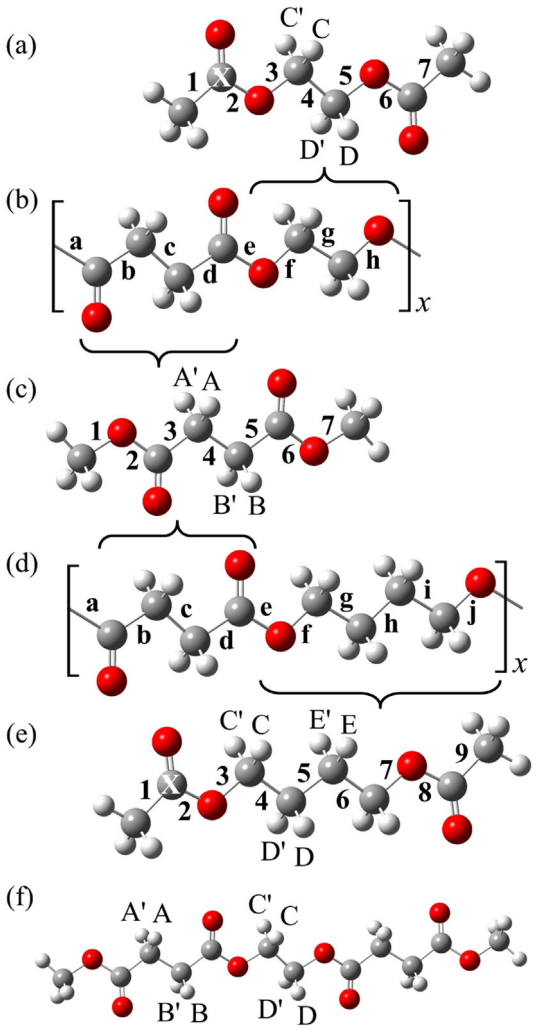

Fig. 1. Polymers and model compounds treated herein: (a) ethylene glycol diacetate (EGDA); (b) poly(ethylene succinate) (PES); (c) dimethyl succinate (DMS); (d) poly(-butylene succinate) (PBS); (e) butylene glycol diacetate (BGDA); (f) ethylene glycol di(methyl succinate) (EGDMS). The repeating units of PES and PBS have been divided into the model compounds as shown and treated here. The red, dark gray, and light gray spheres represent oxygen, carbon, and hydrogen atoms, respectively. The skeletal bonds are numbered or termed as indicated, and *x* is the degree of polymerization. The methylene hydrogen and carbonyl carbon atoms are partly designated as A, A′, B, B′, C, C′, D, D′, E, E′, and X to define NMR spin systems, and the atomic nomenclature is common to Fig. 4 and Table 1, Tables S1, S2, and S3 (Supplementary data). (For interpretation of the references to color in this figure legend, the reader is referred to the web version of this article.)

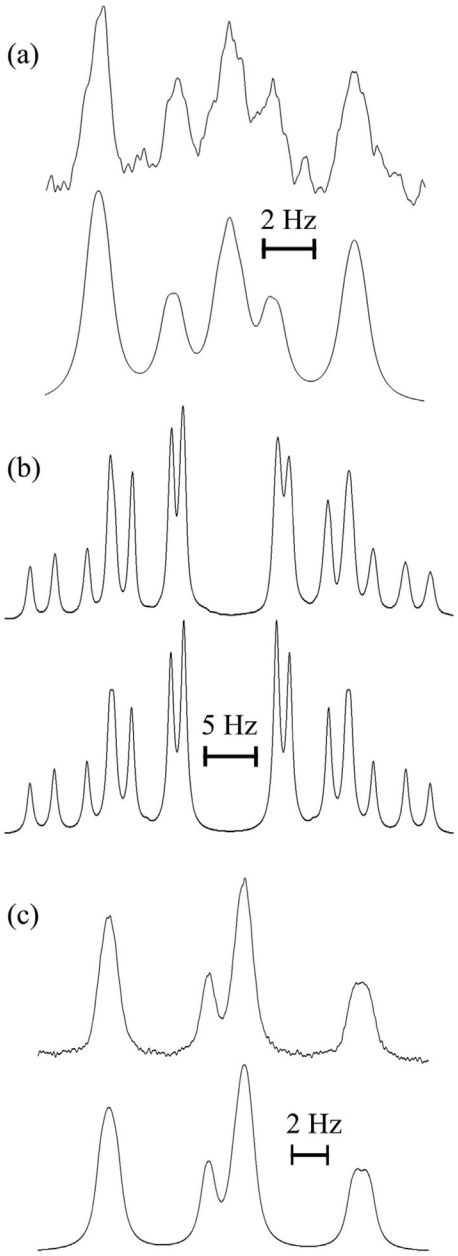

Fig. 2. Observed (above) and calculated (below) ^{1}H NMR spectra of EGDMS and DMS in benzene-d_6 at 25 °C: protons (a) CC′DD′ (satellite peaks) and (b) AA′BB′ of EGDMS; (c) protons AA′BB′ (satellite peaks) of DMS. For the nomenclature of hydrogen atoms, see Figs. 1 and 4. The gNMR simulations yielded $^{3}J_{AB} = 5.63$, $^{3}J_{A'B} = 7.71$, $^{3}J_{CD} = 6.59$, and $^{3}J_{C'D} = 2.87$ Hz for EGDMS and $^{3}J_{AB} = 5.60$ and $^{3}J_{A'B} = 7.78$ Hz for DMS. The vicinal coupling constants of EGDMS and DMS dissolved in different solvents at 15–55 °C are tabulated in Table S1 (Supplementary data).

used: free energy in kcal mol^{-1} (1 kcal mol^{-1} = 4.184 kJ mol^{-1}); bond length in Å (1 Å = 10^{-10} m).

3. Results

3.1. NMR of DMS, EGDA, and EGDMS

As a model for the repeating unit of PES, we first adopted ethylene glycol di(methyl succinate) (EGDMS, Fig. 1f). Next, we have divided the repeating unit at the ester linkage into two subunits, which may be represented by two smaller models: dimethyl succinate (DMS, Fig. 1c) and ethylene glycol diacetate (EGDA, Fig. 1a). These model compounds and EGDA-^{13}C, one of whose carbonyl carbons is selectively labeled by carbon-13, were prepared and underwent ^{1}H and ^{13}C NMR measurements with different solvents at 15–55 °C, and the typical spectra are shown in Figs. 2 and 3. All the spectra were simulated with the gNMR program to yield chemical shifts and coupling constants, and the calculated spectra (below) are compared with the corresponding observations (above) in Figs. 2 and 3. Of the NMR data thus obtained, vicinal ^{1}H–^{1}H and ^{13}C–^{1}H coupling constants (^{3}J's) used to derive bond conformations are listed in Tables S1 and S2 (Supplementary data). The capital alphabetic subscripts (A, A′, B, B′, *etc.*) on the ^{3}J's represent the coupled nuclei, which are illustrated in Figs. 1 and 4.

Mathematical expressions to determine the bond conformations from the observed vicinal coupling constants are listed in

Please cite this article in press as: Sasanuma Y, et al., Conformational characteristics and configurational properties of poly(ethylene succinate) and poly(butylene succinate) and structure–property–function relationships of representative biodegradable polyesters, Polymer (2014), http://dx.doi.org/10.1016/j.polymer.2014.11.003

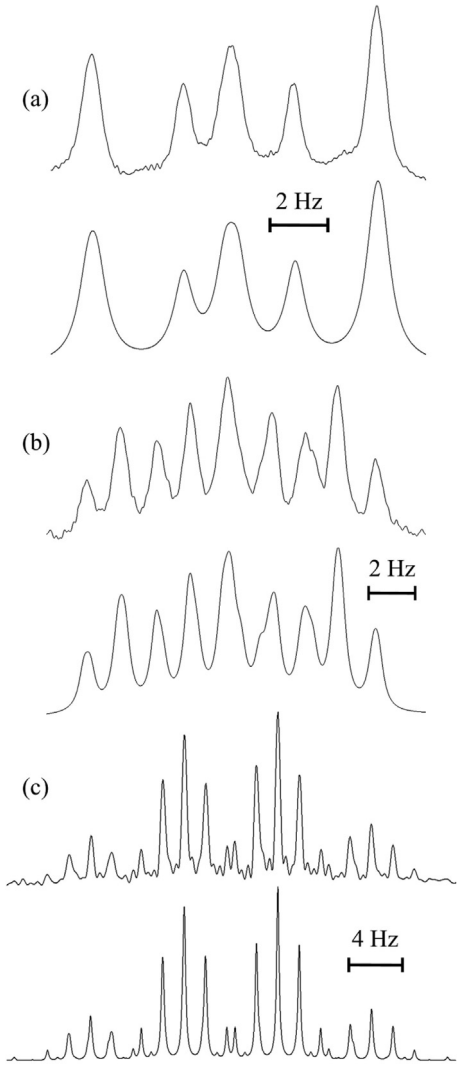

Fig. 3. Observed (above) and calculated (below) ^{1}H and ^{13}C NMR spectra of EGDA and EGDA-^{13}C in methanol-d_4 at 25 °C: (a) protons CC'DD' (satellite peaks) of EGDA; (b) protons CC'DD′ of EGDA-^{13}C; (c) carbon X of EGDA-^{13}C. The spectrum (c) contains a number of small Fourier ripples due to truncation of FID. For the nomenclature of hydrogen and carbon atoms, see Figs. 1 and 4. The gNMR simulations yielded $^{3}J_{XC} = 3.13$, $^{3}J_{CD} = 6.57$, and $^{3}J_{C'D} = 2.88$ Hz. The vicinal coupling constants of EGDA dissolved in different solvents at 15–55 °C are tabulated in Table S2 (Supplementary data).

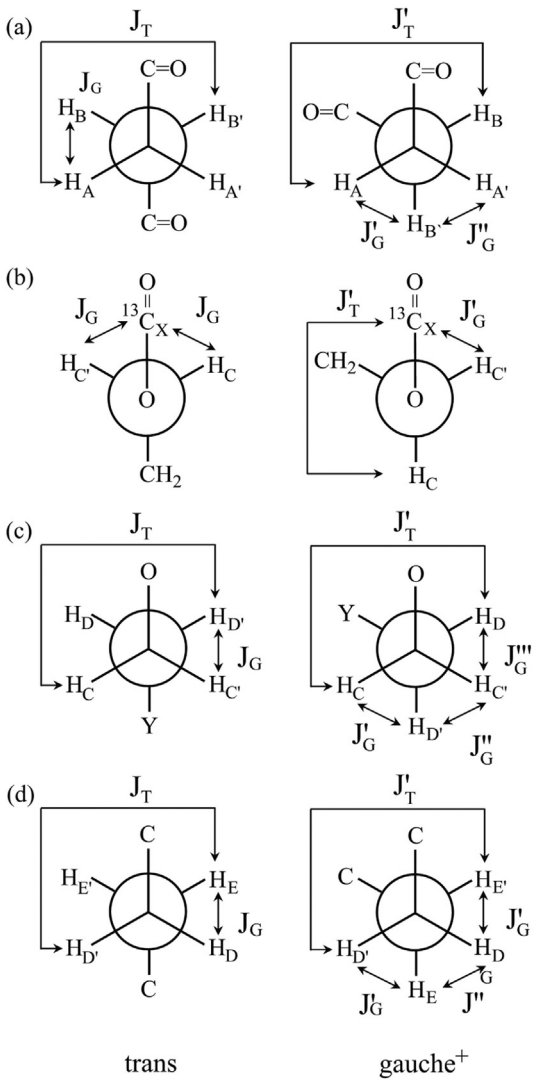

Fig. 4. Newman projections around the (a) $COCH_2-CH_2$, (b) $O-CH_2$, (c) OCH_2-CH_2Y (Y = O or C), and (d) CCH_2-CH_2C bonds, illustrating the coefficients, J_T's and J_G's, used in Table 1.

Table 1. The coefficients, J_T's and J_G's, are based on the experimental values of linear and cyclic compounds including similar bond sequences, a well-established Karplus equation, and MO calculations for the model itself. For the sources, see the footnotes of Table 1. The experimental ^{3}J values were substituted into left-hand sides of the individual equations to yield the p_t and p_g values. Because $p_t + p_g = 1$, only the p_t values are given in Table 2.

In Table 2, the trans fractions of the $COCH_2-CH_2$ bond of DMS range from 0.45 to 0.60 and exactly agree with those of the corresponding bond of EGDMS. The small p_t values (0.05–0.14) of the OCH_2-CH_2O bond of EGDA express a strong gauche preference, being in close agreement with those of EGDMS. These results clearly indicate that the dicarboxylic and diol units, separated by the ester bond, little interfere with each other's conformation and hence can be treated independently. For this reason, we have adopted DMS and EGDA as models for PES rather than EGDMS, because EGDMS is too large to undergo MO calculations.

For the sake of comparison between aliphatic and aromatic esters, the p_t values determined previously from NMR experiments for ethylene glycol dibenzoate (EGDB, $C_6H_5COOCH_2CH_2OCOC_6H_5$), a model compound of poly(ethylene terephthalate) [27], are also shown in Table 2. Both OCH_2-CH_2O and $O-CH_2$ bonds of EGDB exhibit p_t's close to those of EGDA; the outer part, whether aliphatic or aromatic, only a little affects the spacer conformation.

3.2. NMR of BDGA

The above results also permit us to employ DMS and butylene glycol diacetate (BGDA) as model compounds of PBS; therefore, we prepared BGDA and BGDA-^{13}C, carried out NMR measurements, and analyzed the NMR spectra. The typical NMR spectra are shown in Fig. 5, the vicinal coupling constants are listed in Table S3 (Supplementary data), and the mathematical expressions for the analysis are given in Table 1. In Table 3, the p_t values of three bonds of BGDA are compared with those of tetramethylene glycol dibenzoate (TetMGDB, $C_6H_5COO(CH_2)_4OCOC_6H_5$), a model for poly(butylene terephthalate) [28]. Regardless of whether aliphatic or aromatic, both models show similar bond conformations: the OCH_2-CH_2C bond exhibits a moderate gauche preference, and the other two bonds prefer the trans conformation.

Please cite this article in press as: Sasanuma Y, et al., Conformational characteristics and configurational properties of poly(ethylene succinate) and poly(butylene succinate) and structure–property–function relationships of representative biodegradable polyesters, Polymer (2014), http://dx.doi.org/10.1016/j.polymer.2014.11.003

Table 1
Vicinal coupling constants as a function of bond conformations.

Compound	Bond	Equation[a]	J_T's and J_G's (Hz)	Figure
DMS, EGDMS	$COCH_2-CH_2$	$^3J_{AB} = {}^3J_{A'B'} = J_G p_t + [(J'_T + J''_G)/2]p_g$ $^3J_{A'B} = {}^3J_{AB'} = J_T p_t + J'_G p_g$	$J_T = 12.05, J_G = 3.66$ $J'_T = 12.11, J'_G = 1.95, J''_G = 4.70$[b]	4a
EGDA, BGDA	$O-CH_2$	$^3J_{XC} = {}^3J_{XC'} = J_G p_t + [(J'_T + J'_G)/2]p_g$	For EGDA[c] $J_G = 1.7, J'_T = 5.4, J'_G = 4.1$ For BGDA[c] $J_G = 1.7, J'_T = 5.5, J'_G = 3.8$	4b
EGDMS, EGDA, BGDA	OCH_2-CH_2Y	$^3J_{CD} = {}^3J_{C'D'} = J_G p_t + [(J'_T + J''_G)/2]p_g$ $^3J_{C'D} = {}^3J_{CD'} = J_T p_t + (J'_G + J'''_G)p_g$	For EGDMS and EGDA (Y = O)[d] $J_T = 11.4, J_G = 2.3$ $J_T = J'_T, J_G = J'_G = J''_G = J'''_G$ For BGDA (Y = C)[e] $J'_T = 12.3, J'_G = 2.3, J''_G = 1.2, J'''_G = 4.9$ $J_T = J'_T, J_G = (J'_G + J''_G + J'''_G)/3$	4c
BGDA	CCH_2-CH_2C	$^3J_{DE} = {}^3J_{D'E'} = J_G p_t + [(J'_T + J''_G)/2]p_g$ $^3J_{D'E} = {}^3J_{DE'} = J_T p_t + J'_G p_g$	$J'_T = 13.12, J'_G = 3.65, J''_G = 2.96$[f] $J_T = J'_T, J_G = (J'_G + J''_G)/2$	4d

[a] By definition, $p_t + p_g = 1$. Accordingly, the p_t and p_t values derived from the above equations were divided by the sum of p_t and p_g to fulfill $p_t + p_g = 1$.
[b] From MO calculations on DMS at the B3LYP/6-311++G(3df,3pd)//B3LYP/6-311+G(2d,p) level (this study).
[c] From a Karplus equation [23] with the optimized dihedral angles.
[d] Parameters optimized for 1,2-dimethoxyethane and poly(ethylene oxide) [24].
[e] From 1,3-dioxane [25].
[f] From cyclohexane [26].

3.3. MO calculations for DMS, EGDA, and BGDA

According to the above NMR analysis, the repeating unit of PES has been divided into two subunits, succinate and ethylene glycol parts, which may be represented by DMS and EGDA, respectively. To evaluate conformational free energies of PES, we carried out MO calculations for DMS and EGDA. Similarly, conformational free energies of PBS were derived from DMS and BGDA. Because the cis conformation of the C(=O)–O bond has a very high energy [5,6], this bond can be fixed in the trans state. Accordingly, we have defined three internal rotations for DMS and EGDA (bonds 3–5 in Fig. 1a and c) and five for BGDA (bonds 3–7 in Fig. 1e) and adopted the RIS approximation of three states (t, g^+, and g^-); therefore, DMS and EGDA have 27 (3^3) conformers, and BGDA has 243 (3^5). However, the molecular symmetry reduces the number of independent conformers to 10 (DMS and EGDA) and 70 (BGDA). The Gibbs free energies of the irreducible conformers in the gas phase and benzene and chloroform solutions at 25 °C were calculated at the MP2/6-311+G(2d,p) and M062X/6-311+G(2d,p) levels with the geometrical parameters optimized at the B3LYP/6-311+G(2d,p) level. The results are shown in Table 4 (DMS and EGDA) and 5 (BGDA).

For DMS, both MP2 and M062X methods showed the all-trans and tg^+t conformations to be the first and second most stable states, respectively. The ΔG difference between the two conformers seems to be slight: MP2, 0.19–0.26 kcal mol^{-1}; M062X,

Table 2
Trans fractions (p_t's) of DMS, EGDMS, and EGDA, evaluated from NMR and compared with those of ethylene glycol dibenzoate (EGDB).

Solvent	Temp (°C)	DMS	EGDMS		EGDA	
		$COCH_2-CH_2$	$COCH_2-CH_2$	OCH_2-CH_2O	OCH_2-CH_2O	$O-CH_2$
C_6D_{12}	15	0.49			0.11	0.44
	25	0.48			0.12	0.44
	35	0.47			0.12	0.44
	45	0.46			0.13	0.42
	55	0.45			0.14	0.41
C_6D_6	15	0.59	0.59	0.05	0.05	0.53
	25	0.59	0.58	0.06	0.07	0.53
	35	0.56	0.55	0.07	0.08	0.52
	45	0.55	0.55	0.09	0.09	0.51
	55	0.54	0.54	0.10	0.10	0.50
$CDCl_3$	15				0.07	0.56
	25				0.07	0.54
	35				0.09	0.54
	45				0.09	0.53
	55				0.10	0.52
CD_3OD	15	0.60	0.61	0.05	0.06	0.54
	25	0.59	0.58	0.07	0.06	0.53
	35	0.58	0.58	0.07	0.07	0.52
	45	0.56	0.56	0.08	0.08	0.49
	55	0.55	0.55	0.09	0.08	0.49
					EGDB[a]	
C_6D_{12}	25				0.12	0.43
C_6D_6	25				0.08	0.46
CD_3OD	25				0.06	0.41
$(CD_3)_2SO$	25				0.05	0.48

[a] From conformational analysis of poly(ethylene terephthalate) [27].

Please cite this article in press as: Sasanuma Y, et al., Conformational characteristics and configurational properties of poly(ethylene succinate) and poly(butylene succinate) and structure–property–function relationships of representative biodegradable polyesters, Polymer (2014), http://dx.doi.org/10.1016/j.polymer.2014.11.003

0.61–0.73 kcal mol^{-1}. In general, the M062X method yields somewhat larger ΔG's than MP2. For EGDA, both methods determined tg$^+$t as the lowest-energy state (ΔG = −1.1 to −1.5 kcal mol^{-1}), while ΔG of ttg$^+$ was obtained as small as 0.3–0.5 kcal mol^{-1} 1,2-Dimethoxyethane and oligomers of ethylene oxide show different ΔG's in the O–CH_2–CH_2–O bonds: in the gas phase, −0.1 to 0.2 kcal mol^{-1} of tg$^+$t and 1.0 to 1.5 kcal mol^{-1} of ttg$^+$ [29]. It is well-known that the ΔG value of tg$^+$t of poly(ethylene oxide) depends largely on medium [24,29,30]. The nonexistent conformers of DMS and EGDA, represented by the blank lines in Table 4, would include repulsive close contacts between the two C=O oxygen atoms and between the C=O and –O– parts.

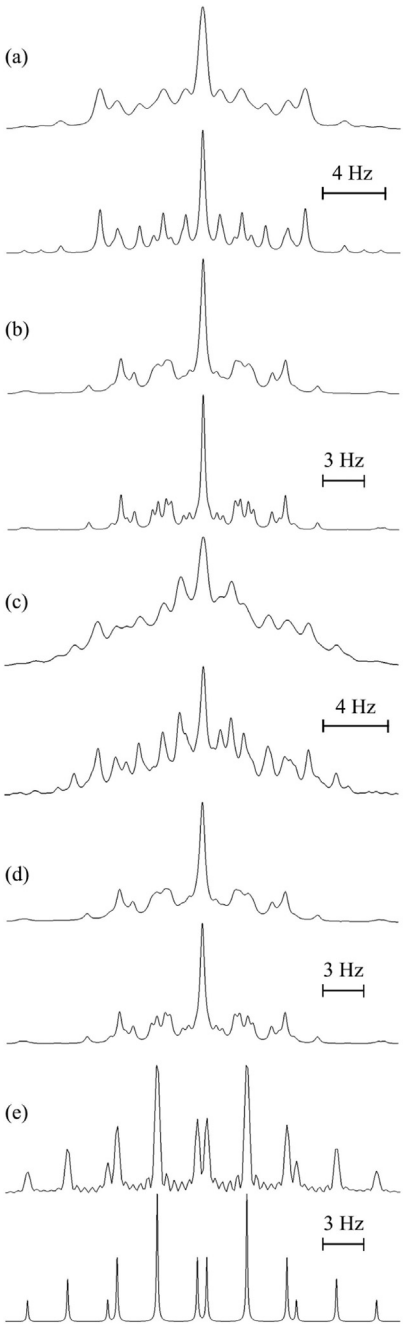

Fig. 5. Observed (above) and calculated (below) ^{1}H and ^{13}C NMR spectra of BGDA and BGDA-^{13}C in cyclohexane-d_{12} at 25 °C: protons (a) CC′ and (b) DD′ (EE′) of BGDA; protons (c) CC′ and (d) DD′ (EE′) of BGDA-^{13}C; (e) carbon X of BGDA-^{13}C. The spectrum (e) includes a number of small Fourier ripples due to truncation of FID. For the nomenclature of hydrogen and carbon atoms, see Figs. 1 and 4. The gNMR simulations yielded $^3J_{XC} = 3.09$, $^3J_{CD} = 6.35$, $^3J_{C'D} = 6.68$, $^3J_{DE} = 5.93$, and $^3J_{D'E} = 9.38$ Hz. The vicinal coupling constants of BGDA dissolved in different solvents at 15–55 °C are tabulated in Table S3 (Supplementary data).

In Table 5, the free energies of 70 conformers of BGDA are listed. Of them, as many as 52 conformers were shown to be existable. Both MP2 and M062X methods predict that the tg$^+$tg$^-$t conformer is the most stable; the ΔG value for the gas phase was obtained as −0.56 kcal mol^{-1} (MP2) and −0.38 kcal mol^{-1} (M062X). The relative stability of this conformer tends to be impaired with an increase in solvent polarity. A number of conformers also show low ΔG's comparable to that of tg$^+$tg$^-$t.

3.4. Comparison between NMR experiments and MO calculations

Bond conformations of DMS, EGDA, and BGDA were calculated from the conformer free energies, and the trans fractions thus obtained are listed for each medium and temperature in Tables 6–8. The trans fractions of the $COCH_2$–CH_2 bond of DMS are 0.48–0.49 (MP2) and 0.57–0.66 (M062X), being found within or partly out of the range of the NMR experiments (0.45–0.60, Table 2). For EGDA, the MP2 and M062X data are close to each other and agree fairly with the NMR observations. Both solvent and temperature effects on the theoretical p_t's are similar to those found in the NMR data: the p_t value of the O–CH_2 bond increases with medium polarity and decreases with increasing temperature. For BGDA, the calculated p_t values agree well with the NMR observations, and the solvent and temperature effects were also reproduced by the MO calculations. In summary, the MP2 and M062X methods yielded results comparable to the NMR observations; however, strictly, the M062X calculations occasionally overestimate the p_t values.

3.5. Refined RIS calculations for PES and PBS

Configurational properties and thermodynamic parameters of PES (PBS) were calculated by statistical mechanics of chain molecules, *i.e.*, what we call, the refined RIS scheme [9], with the conformer free energies of DMS and EGDA (BGDA). Bonds a and e (see Fig. 1b and d) were fixed in the trans state. It has been assumed that intramolecular interaction energies as a function of internal rotations around bonds a–d can be added up in the statistical weight matrix (U_d) of bond d; the U_d matrix was filled with Boltzmann factors of ΔG's of DMS (Table 4) under the 9 × 9 matrix scheme [6], and the U matrices of bonds a–c were filled with unity or null, depending on whether the corresponding conformation exists or not. Similarly, the interaction energies over bonds e–h were accumulated in the U_h matrix, into which Boltzmann factors of ΔG's of EGDA (Table 4) were substituted. For BGDA, the interactions over bonds a–d and e–j have been assumed to be, respectively, expressible by U_d and U_j, which were filled with Boltzmann factors of ΔG's of DMS and BGDA (Table 5) under the 81 × 81 matrix scheme [28]. For mathematical expressions of the U matrices, see Appendix A (Supplementary data). The geometrical parameters used in the RIS calculations are listed in Tables S4 (PES) and S5 (PBS) (Supplementary data).

Table 9 (MP2) and S6 (M062X, Supplementary data) show configurational properties of PES and PBS, derived from the RIS calculations: $\langle r^2\rangle_0/nl^2$, characteristic ratio; $d\ln\langle r^2\rangle_0/dT$, its temperature coefficient; S_{conf}, configurational entropy; U_{conf}, configurational internal energy; p_t trans fraction; $\bar{l}$, $\bar{\theta}$, and $\bar{\phi}$, averaged bond length, bond angle, and dihedral angle, respectively. The characteristic ratios in chloroform at 25 °C was obtained as follows: PES, 6.2 (MP2) and 8.8 (M062X); PBS, 7.1 (MP2) and 8.9 (M062X). The M062X energies yielded larger $\langle r^2\rangle_0/nl^2$ values than the MP2 ones. Inasmuch as the MP2 method reproduced the NMR observations

Please cite this article in press as: Sasanuma Y, et al., Conformational characteristics and configurational properties of poly(ethylene succinate) and poly(butylene succinate) and structure–property–function relationships of representative biodegradable polyesters, Polymer (2014), http://dx.doi.org/10.1016/j.polymer.2014.11.003

Table 3
Trans fractions (p_t's) of BGDA, determined from NMR and compared with those of tetramethylene glycol dibenzoate (TetMGDB).

Solvent	Temp (°C)	O–CH_2	OCH_2–CH_2C	CCH_2–CH_2C
		BGDA		
C_6D_{12}	15	0.54	0.27	0.54
	25	0.53	0.27	0.54
	35	0.52	0.27	0.53
	45	0.52	0.27	0.52
	55	0.51	0.27	0.51
C_6D_6	15	0.58	0.28	0.58
	25	0.56	0.28	0.57
	35	0.56	0.28	0.56
	45	0.55	0.28	0.55
	55	0.55	0.28	0.54
$CDCl_3$	15	0.59	0.28	0.59
	25	0.58	0.28	0.58
	35	0.58	0.28	0.57
	45	0.56	0.28	0.55
	55	0.56	0.28	0.54
CD_3OD	15	0.57	0.27	0.56
	25	0.57	0.27	0.55
	35	0.56	0.27	0.54
	45	0.56	0.27	0.53
	55	0.56	0.27	0.52
$(CD_3)_2SO$	25	0.56	0.28	0.55
	35	0.53	0.28	0.55
	45	0.53	0.28	0.53
	55	0.53	0.28	0.52
		TetMGDB[a]		
C_6D_{12}	25	0.58	0.24	0.53
C_6D_6	25	0.60	0.27	0.57
$CDCl_3$	25	0.62	0.24	0.57
$(CD_3)_2SO$	25	0.60	0.23	0.54

[a] From conformational analysis of poly(butylene terephthalate) [28].

better than M062X, the RIS parameters from the MP2 energies may be more acceptable. The temperature coefficients of PES and PBS are negative irrespective of the energy set. For comparison, the RIS parameters of PLA [6] and PHB [5] are shown in Table 10.

4. Discussion

4.1. Flexibility of polymeric chains

The configurational entropy and configurational internal energy per mole of repeating unit can be calculated from

$$S_{\mathrm{conf}} = \frac{R}{x}\left[\ln Z + T\frac{\mathrm{d}(\ln Z)}{\mathrm{d}T}\right] \quad (1)$$

and

$$U_{\mathrm{conf}} = \frac{RT^2}{x}\frac{\mathrm{d}(\ln Z)}{\mathrm{d}T} \quad (2)$$

where Z is the partition function of the whole chain, an output of the RIS calculation [32,33]. The S_{conf} and U_{conf} values, respectively, correspond to the configurational entropy and intramolecular energy of the Θ state relative to those of the crystal at a given temperature T, and the crystal is assumed to be defect-free; therefore, $S_{\mathrm{cryst}} = 0$ and $U_{\mathrm{cryst}} = 0$.

When we compare the configurational entropy among different polymers, we must divide the S_{conf} value by the number of skeletal bonds in the repeating unit and converted it to that in the unit of cal K^{-1} (mole of bond)$^{-1}$. Herein, the entropy per mole of bond is represented by the lower-case symbol *i.e.*, as s_{conf} The s_{conf} values at the equilibrium melting point T_m^0 of the biodegradable polyesters treated here are 1.25 (PES), 1.46 (PBS), 0.45 (PLA), and 0.96 (PHB) cal K^{-1} (mole of bond)$^{-1}$. Of them, PLA shows the smallest s_{conf}. This can be explained as follows. The repeating unit of PLA has three skeletal bonds, the C(=O)–O bond is essentially fixed in the trans state, degrees of conformational freedom in the other two bonds, O–CH(CH_3)–C(=O), are also extremely restricted by the O···O repulsion and steric hindrance due to the methyl group attached on the asymmetrical carbon, and, consequently, only four conformations are allowed: g^+t, g^+g^+, g^-t, and g^-g^-. Of them, g^-t and g^-g^- are so high in free energy as to occur quite rarely, and hence only two conformations, g^+t and g^+g^+, are the essential sources of conformation- and configuration-dependent properties of PLA [6]. This is the reason for the small s_{conf} of PLA. Similarly, PHB has a chiral center and a methyl side chain, but its repeating unit has four skeletal bonds, which render the PHB chain more flexible than PLA; the s_{conf} value of PHB exceeds double that of PLA. On the other hand, the synthetic polyesters, PES and PBS, being symmetrical chains without pendent group, are so flexible as to yield the large s_{conf}'s. For example, the model for the diol part of PBS, BGDA, is allowed to form as many as 52 conformers, and furthermore, many of the conformers have low free energies comparable to that of the most stable tg^+tg^-t state.

Strictly, it is preferable that the configurational entropy should be evaluated from the ΔG energies at T_m^0; however, the s_{conf} values

Table 4
Conformer free energies of DMS and EGDA.

Conformation[a]			M_k[b]	ΔG (kcal mol^{-1})											
				DMS						EGDA					
				MP2[c]			M062X[d]			MP2[c]			M062X[d]		
				Gas	C_6H_6	$CHCl_3$	Gas	C_6H_6	$CHCl_3$	Gas	C_6H_6	$CHCl_3$	Gas	C_6H_6	$CHCl_3$
t	t	t	1	0.00	0.00	0.00	0.00	0.00	0.00	0.00	0.00	0.00	0.00	0.00	0.00
t	t	g^+	4	0.89	0.80	0.82	1.51	1.40	1.35	0.33	0.42	0.48	0.38	0.46	0.50
t	g^+	t	2	0.19	0.20	0.26	0.73	0.68	0.61	−1.22	−1.35	−1.44	−1.07	−1.32	−1.48
t	g^+	g^+	4	1.18	0.98	0.90	2.05	1.75	1.54	−0.51	−0.55	−0.62	−0.37	−0.53	−0.63
t	g^+	g^-	4												
g^+	t	g^+	2	2.30	2.13	2.11	3.14	2.92	2.82						
g^+	t	g^-	2							0.52	0.79	0.97	0.54	0.77	0.90
g^+	g^+	g^+	2	2.42	2.28	2.42	3.89	3.66	3.54	−0.13	0.04	0.18	−0.16	−0.03	0.06
g^+	g^+	g^-	4							−0.57	−0.27	−0.10	−0.29	−0.06	0.04
g^+	g^-	g^+	2							0.48	0.77	0.88	0.64	0.93	1.04

[a] The blank represents that the local minimum of the potential was not found by the geometrical optimization.
[b] Multiplicity. $\sum_K^{10} M_k = 27$.
[c] At the MP2/6-311+G(2d,p)//B3LYP/6-311+G(2d,p) level.
[d] At the M062X/6-311+G(2d,p)//B3LYP/6-311+G(2d,p) level.

Please cite this article in press as: Sasanuma Y, et al., Conformational characteristics and configurational properties of poly(ethylene succinate) and poly(butylene succinate) and structure–property–function relationships of representative biodegradable polyesters, Polymer (2014), http://dx.doi.org/10.1016/j.polymer.2014.11.003

Table 5
Conformer free energies of BGDA.

Conformation[a]					M_k[b]	ΔG (kcal mol^{-1})					
						MP2[c]			M062X[d]		
						Gas	C_6H_6	$CHCl_3$	Gas	C_6H_6	$CHCl_3$
t	t	t	t	t	1	0.00	0.00	0.00	0.00	0.00	0.00
t	t	t	t	g^+	4	0.49	0.61	0.69	0.53	0.65	0.73
t	t	t	g^+	t	4	−0.14	−0.11	0.02	−0.02	−0.56	0.02
t	t	t	g^+	g^+	4	0.11	0.23	0.39	0.26	0.38	0.43
t	t	t	g^+	g^-	4						
t	t	g^+	t	t	2	0.78	0.77	0.81	0.80	0.80	0.79
t	t	g^+	t	g^+	4	0.89	1.00	1.14	0.99	1.10	1.14
t	t	g^+	t	g^-	4	1.10	1.23	1.36	1.10	1.24	1.34
t	t	g^+	g^+	t	4	0.59	0.63	0.78	0.78	0.81	0.82
t	t	g^+	g^+	g^+	4	0.74	0.89	1.13	0.88	1.03	1.13
t	t	g^+	g^+	g^-	4	0.98	1.19	1.55	1.22	1.41	1.50
t	t	g^+	g^-	t	4	0.27	0.39	0.78	0.51	0.64	0.72
t	t	g^+	g^-	g^+	4						
t	t	g^+	g^-	g^-	4	0.76	1.04	1.53	1.03	1.32	1.50
t	g^+	t	t	g^+	4	−0.27	−0.12	0.14	−0.11	0.03	0.13
t	g^+	t	t	g^-	4	0.07	0.20	0.42	0.25	0.37	0.44
t	g^+	t	g^+	t	2	−0.34	−0.27	0.06	−0.11	−0.06	−0.03
t	g^+	t	g^+	g^+	4	−0.15	0.01	0.34	0.14	0.29	0.37
t	g^+	t	g^+	g^-	4	−0.26	−0.10	0.24	0.10	0.25	0.34
t	g^+	t	g^-	t	2	−0.56	−0.42	−0.13	−0.38	−0.26	−0.19
t	g^+	t	g^-	g^+	4	0.90	1.09	1.41	1.26	1.44	1.54
t	g^+	t	g^-	g^-	4	−0.45	−0.25	0.07	−0.21	−0.02	0.09
t	g^+	g^+	t	g^+	4	0.55	0.74	1.29	0.90	1.09	1.19
t	g^+	g^+	t	g^-	4	0.46	0.64	0.90	0.61	0.79	0.90
t	g^+	g^+	g^+	t	2	−0.35	−0.19	0.15	−0.04	0.10	0.18
t	g^+	g^+	g^+	g^+	4	0.10	0.36	0.71	0.38	0.62	0.77
t	g^+	g^+	g^+	g^-	4	−0.08	0.27	1.35	0.21	0.56	0.72
t	g^+	g^+	g^-	t	4	−0.14	0.05	0.57	0.50	0.69	0.80
t	g^+	g^+	g^-	g^+	4						
t	g^+	g^+	g^-	g^-	4	0.07	0.65	1.30	0.86	1.48	1.84
t	g^+	g^-	t	g^+	4	0.76	0.99	1.31	0.99	1.22	1.36
t	g^+	g^-	t	g^-	4	0.06	0.29	0.74	0.46	0.68	0.82
t	g^+	g^-	g^+	t	2	0.44	0.74	1.11	1.41	1.73	1.92
t	g^+	g^-	g^+	g^+	4						
t	g^+	g^-	g^+	g^-	4						
t	g^+	g^-	g^-	g^+	4						
t	g^+	g^-	g^-	g^-	4	0.67	0.92	1.35	1.08	1.31	1.43
g^+	t	t	t	g^+	2	0.20	0.40	0.54	0.36	0.56	0.66
g^+	t	t	t	g^-	2	0.32	0.59	0.85	0.38	0.66	0.84
g^+	t	t	g^+	g^+	4	0.26	0.52	0.77	0.45	0.72	0.88
g^+	t	t	g^+	g^-	4						
g^+	t	t	g^-	g^+	4	0.72	0.94	1.33	1.01	1.25	1.39
g^+	t	t	g^-	g^-	4	0.46	0.72	1.14	0.68	0.95	1.10
g^+	t	g^+	t	g^+	2	0.85	1.17	1.61	0.97	1.30	1.53
g^+	t	g^+	t	g^-	4	0.79	1.05	1.36	0.87	1.14	1.30
g^+	t	g^+	g^+	g^+	4	0.98	1.19	1.61	1.24	1.46	1.55
g^+	t	g^+	g^+	g^-	4						
g^+	t	g^+	g^-	g^+	4						
g^+	t	g^+	g^-	g^-	4	1.08	1.38	1.79	1.39	1.70	1.88
g^+	t	g^-	t	g^+	2	1.57	1.80	2.09	1.60	1.85	2.00
g^+	t	g^-	g^+	g^+	4	0.97	1.66	2.02	1.62	1.94	2.12
g^+	t	g^-	g^+	g^-	4						
g^+	t	g^-	g^-	g^+	4	0.96	1.38	1.86	1.14	1.57	1.82
g^+	t	g^-	g^-	g^-	4	0.94	1.21	1.56	1.13	1.41	1.56
g^+	g^+	t	g^+	g^+	2	0.19	0.45	0.83	0.61	0.88	1.03
g^+	g^+	t	g^+	g^-	4						
g^+	g^+	t	g^-	g^+	4						
g^+	g^+	t	g^-	g^-	2	−0.05	0.22	0.58	0.23	0.51	0.66
g^+	g^+	g^+	g^+	g^+	2	0.64	0.99	1.45	0.94	1.30	1.50
g^+	g^+	g^+	g^+	g^-	4	0.30	0.83	1.40	0.51	1.05	1.37
g^+	g^+	g^+	g^-	g^+	4						
g^+	g^+	g^+	g^-	g^-	4	0.33	0.78	1.33	1.00	1.46	1.71
g^+	g^+	g^-	g^+	g^+	2	2.96	3.38	3.79	3.56	4.00	4.23
g^+	g^+	g^-	g^+	g^-	4						
g^+	g^+	g^-	g^-	g^+	4						
g^+	g^-	t	g^+	g^-	2						
g^+	g^-	t	g^-	g^+	2	0.39	0.65	1.03	0.86	1.11	1.27
g^+	g^-	g^+	g^+	g^-	4						
g^+	g^-	g^+	g^-	g^+	2						
g^+	g^-	g^-	g^-	g^+	2	0.44	1.13	1.82	0.49	1.19	1.55

[a] The blank represents that the local minimum of the potential was not found by the geometrical optimization.
[b] Multiplicity. $\sum_K^{70} M_{k=1} = 243$.
[c] At the MP2/6-311+G(2d,p)//B3LYP/6-311+G(2d,p) level.
[d] At the M062X/6-311+G(2d,p)//B3LYP/6-311+G(2d,p) level.

Please cite this article in press as: Sasanuma Y, et al., Conformational characteristics and configurational properties of poly(ethylene succinate) and poly(butylene succinate) and structure–property–function relationships of representative biodegradable polyesters, Polymer (2014), http://dx.doi.org/10.1016/j.polymer.2014.11.003

Table 6
Trans fractions (p_t's) of DMS, evaluated from MO calculations.

Medium	Temp (°C)	C(=O)–CH_2		$COCH_2$–CH_2	
		MP2[a]	M062X[b]	MP2[a]	M062X[b]
Gas	15	0.81	0.89	0.49	0.66
	25	0.80	0.89	0.49	0.65
	35	0.79	0.88	0.49	0.64
	45	0.79	0.87	0.49	0.64
	55	0.78	0.86	0.49	0.63
C_6H_6	15	0.78	0.87	0.48	0.63
	25	0.77	0.86	0.48	0.62
	35	0.76	0.85	0.48	0.61
	45	0.76	0.85	0.48	0.61
	55	0.75	0.84	0.48	0.60
$CHCl_3$	15	0.76	0.85	0.49	0.59
	25	0.76	0.85	0.49	0.58
	35	0.75	0.84	0.49	0.58
	45	0.75	0.83	0.48	0.57
	55	0.74	0.82	0.48	0.57

[a] At the MP2/6-311+G(2d,p)//B3LYP/6-311+G(2d,p) level.
[b] At the M062X/6-311+G(2d,p)//B3LYP/6-311+G(2d,p) level.

Table 8
Trans fractions (p_t's) of BDGA, evaluated from MO calculations.

Medium	Temp (°C)	O–CH_2		OCH_2–CH_2C		CCH_2–CH_2C	
		MP2[a]	M062X[b]	MP2[a]	M062X[b]	MP2[a]	M062X[b]
Gas	15	0.52	0.52	0.26	0.31	0.56	0.61
	25	0.52	0.52	0.27	0.31	0.55	0.60
	35	0.52	0.51	0.27	0.32	0.55	0.59
	45	0.51	0.51	0.27	0.32	0.54	0.58
	55	0.51	0.51	0.28	0.32	0.54	0.58
C_6H_6	15	0.57	0.62	0.28	0.35	0.61	0.69
	25	0.56	0.61	0.29	0.35	0.60	0.68
	35	0.56	0.60	0.29	0.35	0.59	0.67
	45	0.55	0.60	0.29	0.35	0.58	0.66
	55	0.55	0.59	0.30	0.35	0.58	0.65
$CHCl_3$	15	0.58	0.59	0.33	0.33	0.67	0.67
	25	0.58	0.59	0.33	0.34	0.66	0.66
	35	0.57	0.58	0.33	0.34	0.65	0.65
	45	0.57	0.58	0.34	0.34	0.64	0.64
	55	0.56	0.57	0.34	0.34	0.64	0.63

[a] At the MP2/6-311+G(2d,p)//B3LYP/6-311+G(2d,p) level.
[b] At the M062X/6-311+G(2d,p)//B3LYP/6-311+G(2d,p) level.

here were calculated from ΔG's at 25 °C. When we calculated the S_{conf} value of poly(ethylene terephthalate) [27] from two sets of ΔG's (at 25 °C and $T_m^0 = 553$ K) and compared the two S_{conf}'s, we found the difference as trifle as 0.3%.

4.2. Intramolecular contribution to melting

The S_{conf} value at T_m^0 represents the intramolecular configurational entropy change during melting, and $S_{conf}/\Delta S_u$ corresponds to the intramolecular contribution to the entropy of fusion (ΔS_u). Some experimental thermal data on PES and PBS have been reported: PES, $T_m^0 = 112.7$ and 114 °C, $\Delta S_u = 16.0$ cal^{-1} K^{-1} mol^{-1}, and $\Delta H_u = 6.20$ kcal mol^{-1} [31,34]; PBS, $T_m^0 = 127.5$, 132, 133.5 and 146.5 °C, $\Delta S_u = 20.3$ and 21.2 cal^{-1} K^{-1} mol^{-1}, and $\Delta H_u = 8.23$ and 8.64 kcal mol^{-1} [31,35,36]. Of them, the data [31] shown in Table 9 have been employed here.

The $S_{conf}/\Delta S_u$ ratios of PES and PBS can be calculated to be 0.62 and 0.69, respectively. Aromatic polyesters of industrial importance have the following $S_{conf}/\Delta S_u$ ratios: poly(ethylene terephthalate), 0.65 [27]; poly(trimethylene terephthalate), 0.65 [28,37]; and poly(butylene terephthalate), 0.75 [28]. These values are close to those of PES and PBS. On the other hand, the $S_{conf}/\Delta S_u$ ratios of PLA and PHB are, respectively, 0.46 and 0.58 [5,6], and PLA has the minimum value among a number of polymers that we have investigated so far. The smallest entropy ratio of PLA is due to its extremely restricted conformational freedom as described above.

Table 7
Trans fractions (p_t's) of EGDA, evaluated from MO calculations.

Medium	Temp (°C)	O–CH_2		OCH_2–CH_2O	
		MP2[a]	M062X[b]	MP2[a]	M062X[b]
Gas	15	0.53	0.55	0.09	0.11
	25	0.52	0.54	0.10	0.12
	35	0.52	0.53	0.10	0.12
	45	0.51	0.52	0.11	0.13
	55	0.50	0.52	0.11	0.13
C_6H_6	15	0.65	0.67	0.08	0.08
	25	0.63	0.66	0.08	0.09
	35	0.62	0.65	0.09	0.09
	45	0.61	0.64	0.09	0.10
	55	0.60	0.63	0.10	0.10
$CHCl_3$	15	0.70	0.72	0.07	0.07
	25	0.69	0.71	0.07	0.07
	35	0.68	0.70	0.08	0.08
	45	0.67	0.69	0.08	0.08
	55	0.66	0.68	0.09	0.09

[a] At the MP2/6-311+G(2d,p)//B3LYP/6-311+G(2d,p) level.
[b] At the M062X/6-311+G(2d,p)//B3LYP/6-311+G(2d,p) level.

4.3. Crystal structures of PES and PBS

The crystal structure of PES was determined as follows: $a = 7.60$ Å, $b = 10.75$ Å, c (fiber axis) = 8.33 Å, orthorhombic space group of $P_{bnb} - D_{2h}^{10}$, and four molecular chains in the unit cell [38]. The conformations of bonds a–h are ttg$^-$tttg$^+$t. Hereafter, we will refer to the part of bonds a–d of PES as DMS moiety and to that of bonds e–h as EGDA moiety. As shown in Table 4, the ttg$^-$t conformation of DMS moiety has a free energy of about 0.2 kcal mol^{-1} (MP2) or 0.6–0.7 kcal mol^{-1} (M062X) relative to that of the all-trans state, and the ttg$^+$t conformation of EGDA moiety is the most stable state of $\Delta G = -1.2$ to -1.4 kcal mol^{-1} (MP2) or -1.1 to -1.5 kcal mol^{-1} (M062X). The outstanding stability of the latter conformation may rule out the possibility of the others in EGDA moiety, and hence DMS moiety would adopt the second most stable ttg$^-$t conformation including an opposite gauche bond to form a pseudoplanar structure and enable the dense chain packing. The dihedral angles of g$^-$ of bond c and g$^+$ of bond g in the crystal were, respectively, determined as $-115°$ ($-109.2°$) and 103° (109.7°), where the parenthetic values were derived from the optimization here at the B3LYP/6-311+G(2d,p) level for DMS and EGDA.

For PBS, two crystal structures are known: α form, $a = 5.23$ Å, $b = 9.12$ Å, c (fiber axis) = 10.90 Å, $\beta = 123.9°$, monoclinic space group of $P_{2_1/n}$, and two molecular chains in the unit cell; β form, $a = 5.84$ Å, $b = 8.32$ Å, c (fiber axis) = 11.86 Å, $\beta = 131.6°$, monoclinic space group of $P_{2_1/n}$, and two molecular chains in the unit cell [39–41]. In the α and β forms, the PBS chain, respectively, adopts the ttttttg$^+$tg$^-$t and all-trans conformations in bonds a–j. Bonds g and i of the α form have dihedral angles of 117.1° (115.7°) and $-117.1°$ ($-115.7°$), respectively, where those optimized here for BGDA are given in the parentheses. The part of bonds a–d of PBS is designated as DMS moiety, and that of bonds e–j as BGDA moiety. The all-trans state of DMS is the lowest in ΔG (Table 4), and the ttg$^+$tg$^-$t conformation in BGDA moiety corresponds to the most stable conformer of BGDA (Table 5) with $\Delta G = -0.6$ to -0.1 kcal mol^{-1} (MP2) or -0.4 to -0.2 kcal mol^{-1} (M062X). The g$^{\pm}$tg$^{\mp}$ conformational trio has often been termed *kink* conformation, which keeps the molecular chain oriented in the fiber-axis direction. In the α form, therefore, both DMS and BGDA moieties are allowed to lie in the most energetically favorable state.

Please cite this article in press as: Sasanuma Y, et al., Conformational characteristics and configurational properties of poly(ethylene succinate) and poly(butylene succinate) and structure–property–function relationships of representative biodegradable polyesters, Polymer (2014), http://dx.doi.org/10.1016/j.polymer.2014.11.003

Table 9
Configurational properties, bond conformations, and averaged geometrical parameters of PES and PBS, evaluated from RIS calculations with MO parameters.[a]

		PES			PBS		
		Gas	$CHCl_3$		Gas	$CHCl_3$	
		25 °C	25 °C	114 °C[b]	25 °C	25 °C	133.5 °C[b]
$<r^2>_0/nl^2$		6.19	6.23	5.43	6.65	7.13	6.26
$d\ln<r^2>_0/dT \times 10^3$ (K^{-1})		−1.9	−2.3	−1.0	−1.4	−1.7	−0.85
S_{conf} (cal K^{-1} mol^{-1})		9.58	9.16	9.96	14.0	14.0	14.6
ΔS_u[c] (cal K^{-1} mol^{-1})				16.0			21.2
U_{conf} (kcal mol^{-1})		0.85	0.81	1.08	1.11	1.16	1.38
ΔH_u[d] (kcal mol^{-1})				6.20			8.64
Trans fraction (p_t)	Bond						
	a	1.00	1.00	1.00	1.00	1.00	1.00
	b	0.80	0.76	0.71	0.80	0.76	0.70
	c	0.49	0.49	0.48	0.49	0.49	0.48
	d	0.80	0.76	0.71	0.80	0.76	0.70
	e	1.00	1.00	1.00	1.00	1.00	1.00
	f	0.52	0.69	0.60	0.52	0.58	0.53
	g	0.10	0.07	0.11	0.27	0.33	0.35
	h	0.52	0.69	0.60	0.55	0.66	0.58
	i				0.27	0.33	0.35
	j				0.52	0.58	0.53
Geometry[e]	Bond	$\bar{l}$	$\bar{\theta}$	$\overline{\phi_{g^+}}$	$\bar{l}$	$\bar{\theta}$	$\overline{\phi_{g^+}}$
	a	1.356	111.1		1.356	111.1	
	b	1.513	112.9	133.7	1.513	112.9	133.7
	c	1.525	112.9	111.2	1.525	112.9	111.2
	d	1.513	111.1	133.7	1.513	111.1	133.7
	e	1.356	116.2		1.356	116.4	
	f	1.441	109.3	92.6	1.447	109.5	91.3
	g	1.508	109.3	111.4	1.520	113.7	115.8
	h	1.441	116.2	92.6	1.533	113.7	112.1
	i				1.520	109.5	115.8
	j				1.447	116.4	91.3

[a] At the MP2/6-311+G(2d,p)//B3LYP/6-311+G(2d,p) level. For the RIS parameters derived from the ΔG energies at the M062X/6-311+G(2d,p) level, see Table S6 (Supplementary data).
[b] The equilibrium melting point [31].
[c] The entropy of fusion [31].
[d] The enthalpy of fusion [31].
[e] The geometrical parameters averaged at 25 °C with the MO energies including the solvent effect of $CHCl_3$. Symbols: $\bar{l}$, averaged bond length (in Å); $\bar{\theta}$, averaged bond angle (in °); $\overline{\phi_{g^+}}$, average dihedral angle (in °) of the g^+ conformation. $\overline{\phi_t} = 0°$ and $\overline{\phi_{g^-}} = -\overline{\phi_{g^+}}$.

The β form appears only under strain [39–41]. Similar stress-induced crystalline transitions were found for poly(ethylene oxide) [42] and poly(butylene terephthalate) [43]. From mechanical properties at the critical stress, the free energy difference between the α and β forms of PBS was estimated to be 0.4 kcal mol^{-1} [40]. Although this value includes both intramolecular and intermolecular factors of the crystalline transition, it falls within our $-\Delta G$ range (0.1–0.6 kcal mol^{-1}) of the tg^+tg^-t conformation of BGDA; therefore, the intermolecular contribution may be slight.

The U_{conf} values of PES and PBS were obtained as positives. This means that the internal energy of the melt is larger by U_{conf} than that of crystalline state: the crystal conformation is more energetically favorable than the Θ state. Our previous study led to a negative U_{conf} for poly(ethylene terephthalate) [27]. This anomaly is due to that its spacer, O—CH_2—CH_2—O, crystallizes to be the unfavorable all-trans structure with the aid of intermolecular π–π attractions. In the crystal of PES, DMS moiety adopts the second stable conformation, while EGDA moiety is allowed to lie in the most stable state. In crystallization of PBS, both DMS and BGDA moieties can change to the lowest ΔG structures. In addition, PES and PBS have the moderate $S_{conf}/\Delta S_u$ ratios. For these two polymers, therefore, we can not find any equilibrium thermodynamic factors to retard crystallization. In fact, PES and PBS are known to exhibit relatively rapid crystallization [31].

Table 10
Configurational properties and thermodynamic quantities of poly(L-lactide) (PLA) and poly((*R*)-3-hydroxybutyrate) (PHB).

	PLA[a]		PHB[b]	
	25 °C	207 °C[c]	25 °C	203 °C[c]
$<r^2>_0/nl^2$	11.84	7.16	5.60	4.24
S_{conf} (cal K^{-1} mol^{-1})	2.02	2.68	2.64	3.84
ΔS_u[d] (cal K^{-1} mol^{-1})		5.83		6.67
U_{conf} (kcal mol^{-1})	0.34	0.61	0.49	0.94
ΔH_u[e] (kcal mol^{-1})		2.80		3.18

[a] From conformational analysis of PLA [6].
[b] From conformational analysis of PHB [5].
[c] The equilibrium melting point.
[d] The entropy of fusion.
[e] The enthalpy of fusion.

4.4. Polymer physicochemical interpretation on microbiological findings

The microbiological findings on the biodegradability of the polyesters [1,10–14], outlined in the Introduction, are discussed here. PHB is a truly natural product that is synthesized and decomposed intracellularly and extracellularly; it is natural that a number of microorganisms can accept and degrade PHB. In the previous paper [5], we elucidated the interaction between PHB and a depolymerase extracted from *Penicillium funiculosum*. The depolymerase has an active site suitable to the (*R*)-enantiomer of 3-hydroxybutyrate. On the other hand, PES and PBS are artificial products that are in principle unaccepted by the environment. Nevertheless, both PES and PBS are biodegradable, because these polyesters may happen to adapt their shapes to the active site of, *e.g.*, lipases. Fig. 6a shows a lipase, *Fusarium solani* cutinase,

Please cite this article in press as: Sasanuma Y, et al., Conformational characteristics and configurational properties of poly(ethylene succinate) and poly(butylene succinate) and structure–property–function relationships of representative biodegradable polyesters, Polymer (2014), http://dx.doi.org/10.1016/j.polymer.2014.11.003

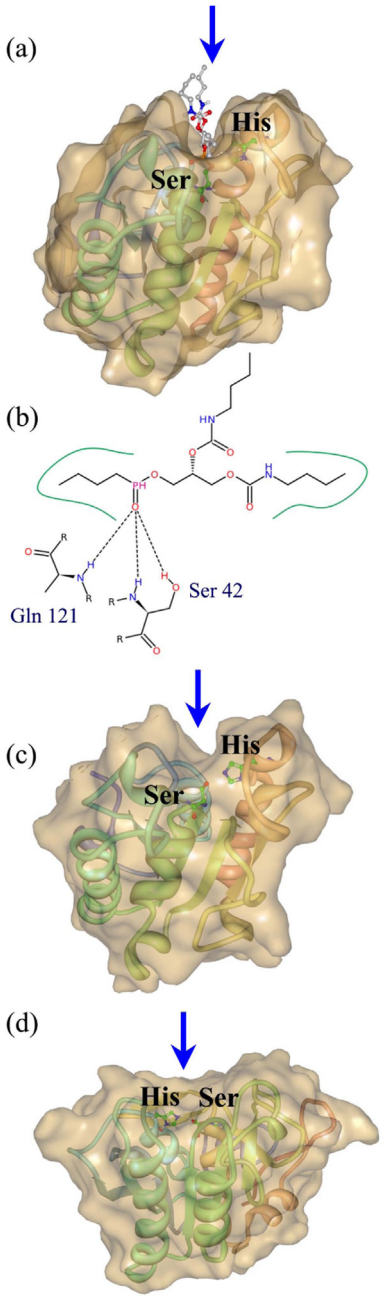

Fig. 6. Crystal structures of degradative enzymes: (a) *Fusarium solani* cutinase (lipase) inhibited by a triglyceride analog (Protein Data Bank (PDB) ID: 1OXM) [44]; (b) its oxyanion hole (Ser 42 and Gln 121) capturing the inhibitor; (c) *Aspergillus oryzae* cutinase (lipase) (PDB ID: 3GBS) [45]; (d) proteinase K (serine protease) extracted from *Tritirachium album limber* (PDB ID: 1IC6) [46]. The crystal structures stored in the Protein Data Bank were visualized by the Molecular Biology Toolkit (Protein Workshop) software [47]. The vertical arrow indicates the active site, and the inner part represented by the ball-and-stick model corresponds to the catalytic serine and histidine residues. The surface texture was simulated by the euclidean distance transform [48], and the oxyanion–inhibitor interaction was depicted by the PoseView software [49].

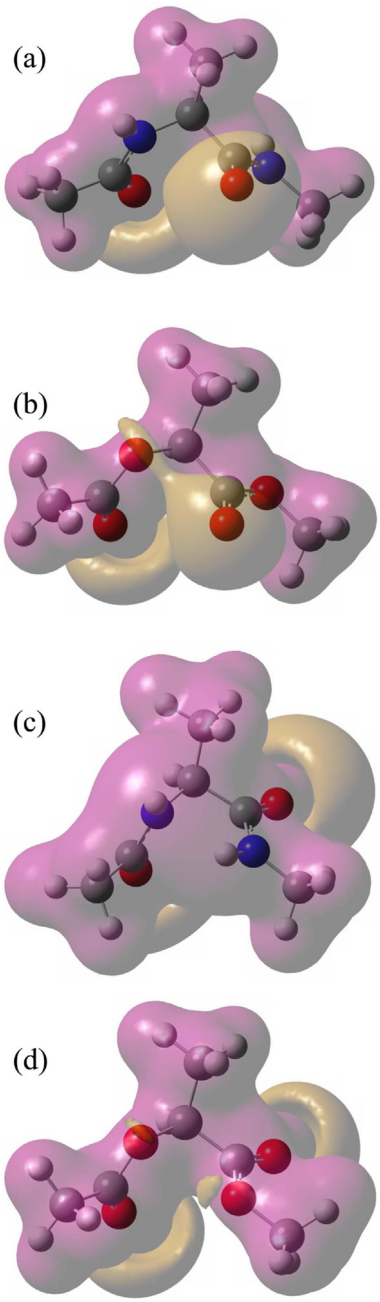

Fig. 7. Most stable conformers of unfolded alanine dipeptide (Ala model) and (*S*)-methyl 2-acetoxypropanoate (lactic acid (LA) model) with the electrostatic potential charge distribution: (a) g^+t (ε_L or polyproline II conformation) of Ala model at (110°, −50°); (b) g^+t of LA model at (107.6°, −15.9°); (c) g^+g^+ (α_L conformation) of Ala model at (105°, 160°); (d) g^+g^+ of LA model at (106.9°, 165.1°) The dihedral angles (ϕ, ψ) defined for the N–CH (or O–CH) and CH–C(=O) bonds respectively, are given in the parentheses.

inhibited by a triglyceride analog [44]. The inhibitor is embedded in the narrow active-site crevice indicated by the arrow. Fig. 6b schematically illustrates the way in which the oxyanion hole of Ser 42 and Gln 121 of the lipase captures the inhibitor. If the O–PH=O part is replaced by an ester group, the illustration would show the interaction between a polyester and the lipase. Fig. 6c shows the crystal structure of a lipase, *Aspergillus oryzae* cutinase [45]. The arrow indicates its active-site crevice, which appears to be somewhat wider than the above but still narrow. For the enzymatic hydrolysis, the molecular chain is required to be completely embedded in the fissure and reach the catalytic site. The PBS chain has neither asymmetric carbon nor side chain and prefers slender conformations: DMS moiety tends to be all-trans, and BGDA moiety will choose its form out of a number of elongated conformations with small ΔG's. Accordingly, the PBS chain may fit itself in the narrow crevice and interact with the active site. However, the asymmetric PLA chain that adopts either tg^+t or tg^+g^+

Please cite this article in press as: Sasanuma Y, et al., Conformational characteristics and configurational properties of poly(ethylene succinate) and poly(butylene succinate) and structure–property–function relationships of representative biodegradable polyesters, Polymer (2014), http://dx.doi.org/10.1016/j.polymer.2014.11.003

conformation is so rigid, distorted, and thick as to be incapable of accessing the crevice of lipases.

Proteinase K is a serine protease, in which a serine residue serves as the nucleophilic center at the active site. It has been suggested that the enzyme tends to selectively cleave the Ala–Ala bond in silk fibroins [11]. Fig. 6d shows proteinase K extracted from *Tritirachium album limber* [46]. The active site of the enzyme is located at the center of a basin rather than a crevice; therefore, the PLA chain may access the central area in spite of its distorted and thick shape.

Recent studies on polypeptides [50–53] have investigate the conformational preference of the Ala residue free from the α-helical and β-sheet structures. It has been pointed out that the Ramachandran diagram of polyalanine [32,54] is not directly applicable to the conformational distribution of the unfolded Ala unit, and that the most populated state of the free Ala residue is the ε_L (polyproline II) conformation (see Fig. 7a); the existing probability was estimated to be 79% [52]. The dihedral angles ($\phi = 110°$, $\psi = -50°$) are comparable to those (107.6°, −15.9°) of the most stable g^+t conformation (Fig. 7b) of (*S*)-methyl 2-acetoxypropanoate, a lactic acid model [6], whose second most stable g^+g^+ state (Fig. 7d) formed at (106.9°, 165.1°) is similar to the α_L conformation (Fig. 7c) at (105°, 160°) of Ala. The lactic acid and Ala units have common configurational features such as the asymmetric carbon, methyl side chain, and the number of skeletal bonds. In addition, as shown above, both units are also so similar in conformational preference and electrostatic potential charge distribution as to undergo the hydrolytic cleavage by the serine protease; that is, proteinase K can not discriminate between lactic acid and Ala units and hence may degrade PLA in mistake for a polypeptide chain.

Such selective affinities between the depolymerases and polyesters are expected to be proved by, *e.g.*, high-resolution single crystal X-ray diffraction experiments for the enzymes complexed with the oligomeric esters: lipase and oligo(butylene succinate); proteinase K and oligo(lactic acid), as demonstrated for PHB [55]. The experiments may provide vivid evidence that the active site of the degradative enzyme selectively interacts with the oligomer fitting the crevice- or basin-like surface.

The equilibrium melting point is related to the enthalpy and entropy of fusion:

$$T_m^0 = \frac{\Delta H_u}{\Delta S_u} \tag{3}$$

If ΔH_u were invariant, T_m^0 would increase with decreasing ΔS_u. For the biodegradable aliphatic polyesters, S_{conf} accounts for 46% (PLA) – 69% (PBS) of ΔS_u. As discussed above, S_{conf} depends on the degree of conformational freedom, which is restricted by the asymmetric carbon, side chain, and short repeating unit and largely affects the interaction with the depolymerase. Therefore, the melting point and enzymatic degradability are subject to the same factors; the two properties are indirectly correlated to each other.

As has been described so far, all the microbiological findings have been satisfactorily interpreted in terms of polymer physicochemistry.

5. Summary

Conformational characteristics of PES and PBS have been investigated by ^1H and ^{13}C NMR experiments and MO calculations on their model compounds and the refined RIS calculations for the polymeric chains. The NMR data showed that the repeating units of PES and PBS can be divided into two parts, dicarboxylic and diol moieties, which can be treated independently of each other; therefore, DMS and EGDA have been employed as the models for PES, and DMS and BGDA for PBS. The MO calculations based on the MP2 and M062X methods with the 6-311+G(2d,p) basis set were carried out for these model compounds, and the MP2 calculations reproduced the NMR observations better than M062X.

The first and second most stable conformers of DMS are ttt and tgt respectively, and the free energy difference between these two states is small (0.2–0.3 kcal mol^{-1}). The former and latter conformations are formed in the C(=O)–CH_2–CH_2–C(=O) bond sequences of crystallized PBS and PES chains, respectively. The most stable conformer of EGDA is tgt that corresponds to the crystal conformation of PES. On the other hand, a number of conformers of BGDA show low free energies, and the lowest-energy tg^+tg^-t conformation is formed in the O–$(CH_2)_4$–O bond sequence of the α crystal of PBS. The β crystal, appearing only under strain, adopts the all-trans structure, which has a little higher free energy (0.1–0.6 kcal mol^{-1}) than tg^+tg^-t.

Configurational entropies per mole of bond, s_{conf}'s, at T_m^0 of the four biodegradable polyesters are 1.46 (PBS), 1.25 (PES), 0.96 (PHB), and 0.45 (PLA) cal K^{-1} (mole of bond)$^{-1}$, expressing the chain rigidity as PBS < PES < PHB ≪ PLA. Characteristic ratios of the polyesters at 25 °C are in the order of PHB (5.60) < PES (6.19) < PBS (6.65) ≪ PLA (11.8). Accordingly, the PLA chain is outstandingly rigid and extended.

The PBS chain is allowed to lie in a number of elongated conformations, adjust itself into the narrow crevice of a lipase, and approach its active site, whereas PLA adopts too distorted tg^+t and tg^+g^+ conformations to be accepted and degraded by lipases. However, the two conformations of PLA are very similar in shape and electrostatic potential charge distribution to stable ε_L (polyproline II) and α_L conformations of the unfolded Ala residue, and hence proteinase K, a serine protease, may degrade PLA in mistake for a polypeptide chain. We expect that the selective affinities between the depolymerases and polyesters will be proved in the future by, *e.g.*, single crystal X-ray diffraction experiments for the enzymes complexed with the oligomeric esters.

As described above, the conformational characteristics and configurational properties of PES and PBS have been elucidated, related to their crystal structures and thermal properties, and compared with those of PHB and PLA. In addition, the microbiological findings regarding the biodegradability of the polyesters have been satisfactorily explained in terms of polymer physicochemistry.

Acknowledgments

This study was partly supported by a Grant-in-Aid for Scientific Research (C) (22550190) from the Japan Society for the Promotion of Science.

Appendix A. Supplementary data

Supplementary data related to this article can be found at http://dx.doi.org/10.1016/j.polymer.2014.11.003.

References

[1] Doi Y, Steinbüchel A, editors. Biopolymers: volume 3b polyesters II properties and chemical synthesis. Weinheim, Germany: Wiley-VCH; 2002.
[2] Aurus R, Lim L-T, Selke SEM, Tsuji H, editors. Poly(lactic acid): synthesis, structures, properties, processing, and applications. Hoboken, New Jersey: Wiley & Sons; 2010.
[3] Carothers WH, Arvin JA. Studies on polymerization and ring formation. ii. poly-esters. J Am Chem Soc 1929;51:2560–70.
[4] Fujimaki T. Processability and properties of aliphatic polyesters, 'bionolle', synthesized by polycondensation reaction. Polym Degrad Stab 1998;59:209–14.

Please cite this article in press as: Sasanuma Y, et al., Conformational characteristics and configurational properties of poly(ethylene succinate) and poly(butylene succinate) and structure–property–function relationships of representative biodegradable polyesters, Polymer (2014), http://dx.doi.org/10.1016/j.polymer.2014.11.003

[5] Sasanuma Y, Katsumata S. Elucidation of conformational characteristics and configurational properties of poly((*r*)-3-hydroxybutyrate) by ab initio statistical mechanics. Polym J 2013;45:727–37.
[6] Sasanuma Y, Touge D. Configurational statistics of poly(L-lactide) and poly(DL-lactide). Polymer 2014;55:1901–11.
[7] Flory PJ. Statistical mechanics of chain molecules. New York: Wiley & Sons; 1969.
[8] Mattice WL, Suter UW. Conformational theory of large molecules: the rotational isomeric state model in macromolecular systems. New York: Wiley-Interscience; 1994.
[9] Sasanuma Y, Asai S, Kumagai R. Conformational characteristics and configurational properties of poly(ethylene oxide-*alt*-ethylene sulfide). Macromolecules 2007;40:3488–97.
[10] Pranamuda H, Tokiwa Y. Degradation of poly(L-lactide) by strains belonging to genus *amycolatopsis*. Biotechnol Lett 1999;21:901–5.
[11] Pranamuda H, Tsuchii A, Tokiwa Y. Poly(L-lactide)-degrading enzyme produced by *amycolatopsis* sp. Macromol Biosci 2001;1:25–9.
[12] Tokiwa Y, Jarerat A. Microbial degradation of aliphatic polyesters. Macromol Symp 2003;201:283–9.
[13] Tokiwa Y, Calabia BP. Degradation of microbial polyesters. Biotechnol Lett 2004;26:1181–9.
[14] Tokiwa Y, Calabia BP, Ugwu CU, Aiba S. Biodegradability of plastics. Int J Mol Sci 2009;10:3722–42.
[15] Bogert MT, Slocum EM. The preparation of various aliphatic halides and halohydrin compounds. J Am Chem Soc 1924;46:763–8.
[16] van den Brand J, Blajiev O, Beentjes PC, Terryn H, de Wit JHW. Interaction of ester functional groups with aluminum oxide surfaces studied using infrared reflection absorption spectroscopy. Langmuir 2004;20:6318–26.
[17] Budzelaar PH. gNMR, version 5.0. Letchworth, U.K: IvorySoft & Adept Scientific plc; 2004.
[18] Frisch MJ, Trucks GW, Schlegel HB, Scuseria GE, Robb MA, Cheeseman JR, et al. Gaussian 09 Revision B.01. Wallingford CT: gaussian Inc; 2009.
[19] Zhao Y, Truhlar DG. Density functionals with broad applicability in chemistry. Acc Chem Res 2008;41:157–67.
[20] Helgaker T, Watson M, Handy NC. Analytical calculation of nuclear magnetic resonance indirect spin–spin coupling constants at the generalized gradient approximation and hybrid levels of density-functional theory. J Chem Phys 2000;113:9402–9.
[21] Cancès E, Mennucci B, Tomasi J. A new integral equation formalism for the polarizable continuum model: theoretical background and applications to isotropic and anisotropic dielectrics. J Chem Phys 1997;107:3032–41.
[22] (the "Gold Book"). In: McNaught AD, Wilkinson A, editors. IUPAC. Compendium of chemical terminology. 2nd ed. Oxford, UK: Blackwell Scientific Publications; 1997.
[23] Tvaroška I, Hricovíni M, Petráková E. An attempt to derive a new Karplus-type equation of vicinal proton–carbon coupling constants for C–O–C–H segments of bonded atoms. Carbohydr Res 1989;189:359–62.
[24] Tasaki K, Abe A. NMR studies and conformational energy calculations of 1,2-dimethoxyethane and poly(oxyethylene). Polym J 1985;17:641–55.
[25] Anteunis MJO, Tavernier D, Borremans F. A review on the conformational aspects in the 1,3-dioxane system. Heterocycles 1976;4:293–371.
[26] Edgar J, Garbisch W, Griffith MG. Proton couplings in cyclohexane. J Am Chem Soc 1968;90:6543–4.
[27] Sasanuma Y. Conformational characteristics, configurational properties, and thermodynamic characteristics of poly(ethylene terephthalate) and poly(-ethylene-2,6-naphthalate). Macromolecules 2009;42:2854–62.
[28] Sasanuma Y, Wagai Y, Suzuki N, Abe D. Conformational characteristics and configurational properties of poly(butylene terephthalate) and structure-property relationships of aromatic polyesters. Polymer 2013;54:3904–13.
[29] Sasanuma Y, Sugita K. The attractive gauche effect of ethylene oxides. Polym J 2006;38:983–8.
[30] Sasanuma Y, Ohta H, Touma I, Matoba H, Hayashi Y, Kaito A. Conformational characteristics of poly(ethylene sulfide) and poly(ethylene oxide): solvent dependence of attractive and repulsive gauche effects. Macromolecules 2002;35:3748–61.
[31] Papageorgiou GZ, Bikiaris DN. Crystallization and melting behavior of three biodegradable poly(alkylene succinates). a comparative study. Polymer 2005;46:12081–92.
[32] Brant DA, Miller WG, Flory PJ. Conformational energy estimates for statistically coiling polypeptide chains. J Mol Biol 1967;23:47–65.
[33] Sasanuma Y, Watanabe A, Tamura K. Structure-property relationships of polyselenoethers $[-(CH_2)_ySe-]_x$ ($y = 1$, 2, and 3) and related polyethers and polysulfides. J Phys Chem B 2008;112:9613–24.
[34] Lu H-Y, Peng J-S, Chen M, Chang W-C, Chen CH, Tsai C-J. Characterization, crystallization kinetics and melting behavior of poly(ethylene succinate-*co*-21 mol% trimethylene succinate) copolyester. Eur Polym J 2007;43:2630–40.
[35] Miyata T, Masuko T. Crystallization behavior of poly(tetramethylene succinate). Polymer 1998;39:1399–404.
[36] Gan Z, Abe H, Kurokawa H, Doi Y. Solid-state microstructures, thermal properties, and crystallization of biodegradable poly(butylene succinate) (pbs) and its copolyesters. Biomacromolecules 2001;2:605–13.
[37] Sasanuma Y, Suzuki N. Influence of weak attractive interactions on structures and properties of poly(trimethylene terephthalate). Macromolecules 2009;42:7203–12.
[38] Ueda AS, Chatani Y, Tadokoro H. Structural studies of polyesters. iv. molecular and crystal structures of poly(ethylene succinate) and poly(ethylene oxalate). Polym J 1971;2:387–97.
[39] Ichikawa Y, Suzuki J, Washiyama J, Moteki Y, Noguchi K, Okuyama K. Strain-induced crystal modification in poly(tetramethylene succinate). Polymer 1994;35:3338–9.
[40] Ichikawa Y, Washiyama J, Moteki Y, Noguchi K, Okuyama K. Crystal transition mechanisms in poly(tetramethylene succinate). Polym J 1995;27:1230–8.
[41] Ichikawa Y, Kondo H, Igarashi Y, Noguchi K, Okuyama K, Washiyama J. Crystal structures of α and β forms of poly(tetramethylene succinate). Polymer 2000;41:4719–27.
[42] Takahashi Y, Sumita I, Tadokoro H. Structural studies of polyethers. ix. Planar zigzag modification of poly(ethylene oxide). J Polym Sci Polym Phys Ed 1973;11:2113–22.
[43] Tashiro K, Nakai Y, Kobayashi M, Tadokoro H. Solid-state transition of poly(-butylene terephthalate) induced by mechanical deformation. Macromolecules 1980;13:137–45.
[44] Longhi S, Mannesse M, Verheij HM, de Haas GH, Egmond M, Knoops-Mouthuy E, et al. Crystal structure of cutinase covalently inhibited by a triglyceride analogue. Protein Sci 1997;6:275–86.
[45] Liu Z, Gosser Y, Baker PJ, Ravee Y, Lu Z, Alemu G, et al. Structural and functional studies of *aspergillus oryzae* cutinase: enhanced thermostability and hydrolytic activity of synthetic ester and polyester degradation. J Am Chem Soc 2009;131:15711–6.
[46] Betzel C, Gourinath S, Kumar P, Kaur P, Perbandt M, Eschenburg S, et al. Structure of a serine protease proteinase k from *tritirachium album limber* at 0.98 Å resolution. Biochemistry 2001;40:3080–8.
[47] Moreland JL, Gramada A, Buzko OV, Zhang Q, Bourne PE. The molecular biology toolkit (mbt): a modular platform for developing molecular visualization applications. BMC Bioinforma 2005;6:21.
[48] Xu D, Zhang Y. Generating triangulated macromolecular surfaces by euclidean distance transform. PloS One 2009;4:e8140.
[49] Stierand K, Rarey M. Drawing the pdb: protein–ligand complexes in two dimensions. Med Chem Lett 2010;1:540–5.
[50] Shi Z, Olson CA, Rose GD, Baldwin RL, Kallenbach NR. Polyproline ii structure in a sequence of seven alanine residues. Proc Natl Acad Sci U S A 2002;99:9190–5.
[51] Schweitzer-Stenner R. Distribution of conformations sampled by the central amino acid residue in tripeptides inferred from amide i band profiles and NMR scalar coupling constants. J Phys Chem B 2009;113:2922–32.
[52] Hagarman A, Measey TJ, Mathieu D, Schwalbe H, Schweitzer-Stenner R. Intrinsic propensities of amino acid residue in g × g peptides inferred from amide i′ band profiles and NMR scalar coupling constants. J Am Chem Soc 2010;132:540–51.
[53] Parchaňský V, Kapitán J, Kaminský J, Šebestík J, Bouř P. Ramachandran plot for alanine dipeptide as determined from Raman optical activity. Phys Chem Lett 2013;4:2763–8.
[54] Pullman B. Proteins, nucleic acids and their constituents. In: Pullman B, editor. Quantum mechanics of molecular conformations. London: John Wiley & Sons; 1976. p. 295–383 [Ch. 4].
[55] Hisano T, Kasuya K, Tezuka Y, Ishii N, Kobayashi T, Shiraki M, et al. The crystal structure of polyhydroxybutyrate depolymerase from *Penicillium funiculosum* provides insights into the recognition and degradation of biopolyesters. J Mol Biol 2006;356:993–1004.

Please cite this article in press as: Sasanuma Y, et al., Conformational characteristics and configurational properties of poly(ethylene succinate) and poly(butylene succinate) and structure–property–function relationships of representative biodegradable polyesters, Polymer (2014), http://dx.doi.org/10.1016/j.polymer.2014.11.003